

SELECTION EFFECTS IN HIGH-REDSHIFT SUBMILLIMETER SURVEYS AND POINTED OBSERVATIONS

ANDREW W. BLAIN

Institute of Astronomy, Madingley Road, Cambridge, CB3 0HA, UK

E-mail: awb@ast.cam.ac.uk

The results of the first generation of submillimeter (submm)-wave surveys have been published. The opening of this new window on the distant Universe has added considerably to our understanding of the galaxy formation process, by revealing a numerous population of very luminous distant galaxies. Most would have been very difficult to identify using other methods. The potential importance of selection effects, especially those connected with the spectral energy distributions (SEDs) of the detected galaxies, for the interpretation of the results are highlighted.

1 Introduction

From the *IRAS* survey, it was clear that the absorption and re-emission of starlight by interstellar dust in the Milky Way, and of both starlight and accretion energy from AGN by dust in external galaxies, is a very important process. The thermal emission spectrum of dust heated by this radiation, which is observed to peak at a wavelength of order $100\ \mu\text{m}$, is redshifted into the submm waveband with a very strong K -correction, making high-redshift submm galaxies unusually easy to detect as compared with their low-redshift counterparts. Between redshifts of about 0.5 and 10 the K -correction almost balances the cosmological dimming of a source with a fixed template SED, and so the flux density received from a galaxy is approximately constant.¹¹ Although the submm waveband is thus a very attractive window for cosmology,⁷ it is technically very challenging to image submm radiation at the faint sensitivity levels – several mJy at $850\ \mu\text{m}$ – required to detect even an ultraluminous galaxy, defined as possessing a far-infrared(IR) luminosity in excess of $10^{12}\ L_{\odot}$, at any redshift $z \geq 0.5$.

Systematic submm-wave cosmology has only been possible since the commissioning of the SCUBA camera at the James Clerk Maxwell Telescope in 1997.³⁴ A handful of known high-redshift galaxies and AGN were detected earlier using single-pixel detectors,^{15,19,37} but blank-field surveys were impossible, due to a combination of relatively low sensitivity and a very small field of view. SCUBA brought 37 and 91 detectors operating in the atmospheric windows at 850 and $450\ \mu\text{m}$ respectively, providing a 2.5-arcmin field of view, and has been used to good effect to make a range of surveys of the high-

redshift Universe.^{51,36,2,21,3,57,14} Recently, the MAMBO camera at the IRAM 30-m telescope has also produced deep survey images at 1.25 mm.⁵ The existing BIMA, IRAM, Nobeyama and OVRO interferometer arrays are very valuable for making sensitive, high-resolution mm-wave observations, but because of their small fields of view, they are not practical survey instruments. Prior to the debut of SCUBA, the one-dimensional multi-channel 350- μ m SHARC camera at the Caltech Submm Observatory (CSO) was used to limit the counts of faint submm galaxies, and the relatively large primary beam of the BIMA array at 2.8 mm was exploited to impose the first limit to the mm-wave counts in a mosaicked image of the Hubble Deep Field.⁵⁸ The detection of a very significant intensity of submm/far-IR background radiation from the *COBE* FIRAS and DIRBE datasets was achieved in parallel to the first SCUBA surveys.^{47,49,33,25}

The prospects for further instrumental developments are excellent. The lithographic manufacture of large arrays of bolometers is now routinely demonstrated.¹² The BOLOCAM detector array³⁰ that uses one type of this technology has recently undergone its first engineering tests at the CSO. An alternative technology is exploited in the forthcoming SHARC-II¹⁷ camera for the CSO. Bolometers that exploit superconducting and quantum interference devices rather than simple thermistors are also being developed. These promise increased stability and reduced response time, and would lead to a crucial increase in the degree of multiplexing possible in their readouts, and so to much larger arrays. The future SCUBA-II³⁵ camera for the JCMT and large-format bolometer cameras for the 50-m LMT⁵⁰ are expected to exploit such devices. The SMA⁵⁹ interferometer array on Mauna Kea will provide the first sensitive, fully-*uv*-sampled interferometric images in the submm band, and in the future the 64 \times 12 m ALMA array⁶⁰ will provide extremely sensitive, high-resolution observations.

Wide-band mm/submm-wave spectrometers³⁸ are also being developed, using both arrays of heterodyne detectors²⁴ and dispersive techniques.¹⁰ These instruments will offer the potential for the direct determination of redshifts for mm/submm-selected galaxies from mm-wave observations of CO lines. There is a natural symbiotic relationship between new panoramic bolometer cameras^{30,35} and these spectrographs, which together will be capable of both detecting and obtaining redshifts for large samples of high-redshift dusty galaxies without recourse to either optical, near-IR, or even radio telescopes.

The results and consequences of the first SCUBA surveys have been discussed extensively elsewhere.^{8,36,21,43,9,3,44,54} Here the potential selection effects in this new waveband^{21,43,11} are described in the context of our knowledge of the SEDs of the detected objects.

2 Submm-wave selection effects

2.1 Redshifts of submm-selected galaxies

In mm/submm-wave surveys there is a unique bias in favor of the detection of high-redshift galaxies at the expense of their low-redshift counterparts. The flux density of a galaxy *with a fixed SED* is expected to be approximately constant over a wide range of redshifts from about 0.5 to 10. The increase in the volume element out to $z \simeq 2$ conspires to bias the selection function to greater redshifts; a demonstration of this effect in currently popular world models as a function of SED is presented elsewhere.¹¹

There is broad agreement^{44,54} that the objects detected in SCUBA surveys are at redshifts $z \simeq 3 \pm 2$. All three SCUBA galaxies with redshifts confirmed using CO spectroscopy^{26,27,55} are at $z > 1$. Others for which deep multiwaveband data is available^{36,18,52,21,29} have no potential low-redshift counterparts. Four of the first galaxies from the CUDSS survey^{22,43} were identified with galaxies at $z < 1$; however, more extensive results^{21,44} show a smaller fraction of potential low-redshift identifications. Note that two initially plausible low-redshift identifications of galaxies in the SCUBA Lens Survey^{51,53} were subsequently revised upwards in the light of additional data.⁵² New results from this meeting^{57,13} are consistent with a distant redshift distribution.

Despite their potential for detecting high-redshift galaxies, submm surveys detect galaxies at restframe wavelengths considerably longwards of the peak of their SEDs. It is thus possible that the form of this SED can affect the interpretation of the results of SCUBA surveys.^{21,11} The main effect would be to overestimate the bolometric luminosity associated with a submm-selected galaxy if its dust temperature was overestimated.

2.2 SEDs of submm-selected galaxies

Potential selection effects in submm-wave surveys are controlled by the SEDs of the detected galaxies. The SEDs of individual dusty galaxies certainly vary from galaxy to galaxy, and could vary systematically with luminosity and redshift. Here and in previous work connected with the SCUBA Lens Survey,^{8,9,11} three parameters are used to describe the SED; a dust temperature T in a standard Planck function B_ν , an index β in a dust emissivity function ν^β and a spectral index α to describe the mid-IR SED, $f_\nu \propto \nu^\alpha$.

Dust SEDs are steeper than blackbody spectra in the Rayleigh–Jeans (RJ) regime. If the SED is represented by the function $\nu^\beta B_\nu$, then the RJ spectral index is $-2 - \beta$. Some authors^{4,45} represent the SED by a greybody of the form $(1 - \exp -K\nu^\beta)B_\nu$, explicitly taking account of the increase in

optical depth with increasing frequency. In this case, the RJ spectral index is also $-2 - \beta$, but the SEDs differ near their peaks. Temperatures fitted using a greybody SED are typically about 20% greater than those derived from the $\nu^\beta B_\nu$ SED.

The mid-IR α term is introduced because dust SEDs do not fall exponentially like blackbodies in the Wien regime, due to the contribution from additional hot dust components in the interstellar medium. At frequencies above which the gradient of $\nu^\beta B_\nu$ is steeper than that of the power law ν^α , the SED is represented by this power law, thus incorporating the observed mid-IR properties of galaxy SEDs; see Fig. 1. The radio emission associated with dusty galaxies is represented by an additional power-law function, normalized to fit the low-redshift far-IR–radio correlation.¹⁶

These three simple parameters can provide an adequate and appropriate description of the SEDs of distant dusty galaxies from the mm to mid-IR waveband,⁶ which are constrained only by a handful of broad-band photometric measurements with little or no spatial resolution. When sub-arcsecond spatially-resolved images from ALMA are available, it will be important to investigate more details of the mm to near-IR SEDs, using radiative transfer models, including full details of the complex geometry, the different physical components and conditions in a merging, star-forming galaxy, and of a potential point-like nuclear heat source.^{23,32} However, few of the parameters required by such models can be constrained at present, and so we prefer to use the simple three-parameter SED. Based on fits to the form of evolution of low-redshift 60- μm *IRAS* galaxies and more distant galaxies selected at 175 μm , described elsewhere,⁸ values of $T = 38\text{ K}$, $\beta = 1.5$ and $\alpha = -1.7$ were chosen; the associated SED is shown by the dashed line in Fig. 1.

Information about the SEDs of the high-redshift luminous galaxies detected in submm surveys can be obtained by several different routes.

First, submm-wave observations of a representative sample of galaxies from the *IRAS* catalog can be made.²⁰ However, being at low redshifts ($z \leq 0.1$), the properties of these galaxies have rather little overlap with those of the more distant, typically much more luminous galaxies found in deep submm surveys. The results indicate that there is a weak trend for the dust temperature to increase with increasing luminosity, and that $T = 36 \pm 5\text{ K}$ and $\beta = 1.3 \pm 0.2$ are reasonable typical values; see the dotted SED shown in Fig. 1. Independent results for the typical SEDs of *IRAS* galaxies, which yields a similar generic spectrum, are shown by the solid line in Fig. 1.³¹

Secondly, color information for high-redshift submm-selected dusty galaxies can be obtained from multiband submm/mm/IR observations and combined with independent redshift information to derive T and β .^{40,41} The few

temperatures available are in the range 40-50 K, consistent with the SEDs described above. The relevant data are plotted in Fig. 1.^{11,48} Note that because dust SEDs are thermal, it is impossible to distinguish *a priori* between the effects of an increase in temperature or a reduction in redshift.

Thirdly, the color technique can be used to measure SEDs for high-redshift galaxies with known redshifts, but a less uniform selection criterion, for example the most luminous *IRAS* galaxies, high-redshift radio galaxies, optically-selected AGN and gravitational lenses.^{11,48} The ranges of luminosity and redshift that are appropriate to the SCUBA galaxies are sampled using this approach; however, the surveyed objects are diverse, and perhaps extreme and unrepresentative. For example, the dust temperature inferred from observations of the most luminous lensed quasar^{42,6} is about three times greater than the typical temperature inferred from *IRAS*, *ISO* and SCUBA data.

In general, dust temperatures in high-redshift AGN seem to be greater than in *IRAS* and SCUBA galaxies. This is probably due both to the selection effect against detecting hot objects in SCUBA surveys, and to higher intrinsic temperatures in the most luminous objects.

2.3 Pointed observations

There has been much concerted effort to detect statistical samples of known high-redshift galaxies, such as the Lyman-break galaxies,¹³ classical radio galaxies,¹ quasars^{4,39} and gravitational lenses using mm/submm instruments. Before SCUBA, this technique provided the only opportunity to study the high-redshift mm/submm Universe.^{15,19,37} Today, it provides a direct opportunity to connect the results obtained from deep submm surveys to more developed fields of observational cosmology carried out in other wavebands.

The selection functions at work in these studies favor the detection of the highest redshift members of flux-limited samples of objects selected in another waveband, because of the familiar mm/submm *K*-correction. The ratio between the submm flux density of a galaxy and that measured in any other waveband, with the possible exception of soft X-ray observations of highly-enriched gas-rich AGN, is expected to be a strongly increasing function of redshift. For example, the submm-radio/optical flux density ratio of a galaxy with a reasonable radio or optical SED, $f_\nu \propto \nu^{-1}$, and a submm SED, $f_\nu \propto \nu^{3.5}$, should increase with redshift z as $(1+z)^\gamma$, where $\gamma \simeq 4.5$. The SCUBA detection of a $z = 5.8$ quasar discovered in the Sloan Digital Sky Survey reported at this meeting, despite the typical lack of detections of $z \simeq 3$ quasars,³⁹ provides a possible example. It is exciting that the growing number of very high-redshift objects detected in other wavebands could be relatively

easy to detect in pointed mm/submm observations, using existing telescopes like the JCMT and CSO, forthcoming telescopes like the SMA and LMT, and ultimately at great sensitivity and resolution using ALMA. The intergalactic medium is always transparent to mm/submm radiation, and so this type of observation could be very important for tracing the process of re-ionization in the years ahead.

It should be possible to study the intrinsic evolution of the dust emission properties of a well-defined sample of galaxies by making mm/submm observations of a sub-sample that have been selected carefully elsewhere to have a fixed luminosity as a function of redshift.¹ For example, while the fraction of powerful radio galaxies drawn from flux-limited samples that are detected by SCUBA is observed to increase with redshift, consistent with the selection effect above, a sub-sample with matched radio luminosities still displays a statistically significant increase in dust luminosity with redshift, indicating that powerful radio galaxies are systematically more luminous in the submm than the radio waveband at higher redshifts.¹

3 Summary: future observations of very early galaxies

Selection effects in deep mm/submm-wave surveys generally favor the detection of the most distant objects. For a fixed bolometric luminosity, dusty galaxies with colder dust temperatures are more likely to be detected. The detection of galaxies at the highest redshifts in the mm/submm waveband requires only that they are luminous and contain dust. Because absorption along the line of sight is not significant in the mm/submm waveband, dust generated and heated in the very first galaxies, prior to the epoch of re-ionization, could potentially be detected in the submm waveband.

Acknowledgments

I thank the Raymond and Beverly Sackler Foundation for support at the IoA, UMass/INAOE for support at the meeting, the CfA for organizing ‘The First Generation of Cosmic Structures’, for which some of this material was prepared, and Jan and Rick Caldwell for hospitality prior to both meetings.

References

1. E.N. Archibald, *et al*, MNRAS **submitted**, astro-ph/0002083 (2000).
2. A.J. Barger, L.L. Cowie, *et al*, Nature **394**, 247 (1998).
3. A.J. Barger, L.L. Cowie, and D.B. Sanders, ApJ **518**, L5 (1999).

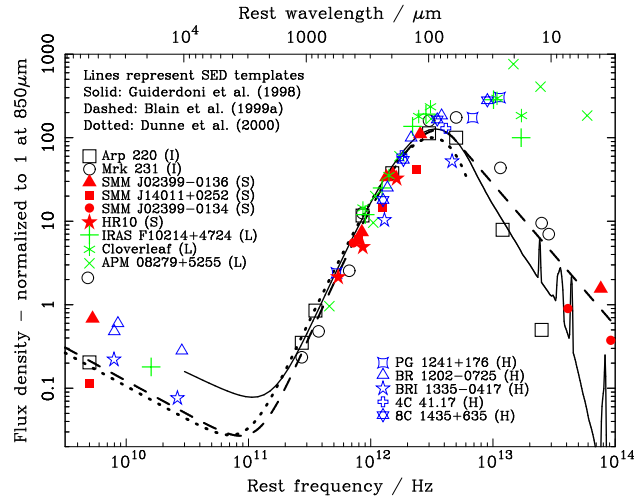


Figure 1. SEDs of a wide range of dusty galaxies with known redshifts, including known lensed sources (L), high-redshift AGN (H), low-redshift *IRAS* galaxies (I) and submm-selected galaxies (S). Three spectral templates are also shown. Only those objects with redshifts and both mid-IR and submm data are plotted. Both the re-normalized data and the templates are very similar at wavelengths longer than $60 \mu\text{m}$.

4. D.J. Benford, P. Cox, *et al*, *ApJ* **518**, L65 (1999).
5. F. Bertoldi, *et al*, *A&A* **in press**, astro-ph/0006094 (2000).
6. A.W. Blain, *MNRAS* **304**, 699 (1999).
7. A.W. Blain, and M.S. Longair, *MNRAS* **264**, 509 (1993).
8. A.W. Blain, I. Smail, R.J. Ivison, *et al*, *MNRAS* **302**, 632 (1999).
9. A.W. Blain, A. Jameson, *et al*, *MNRAS* **309**, 715 (2000).
10. A.W. Blain, D.T. Frayer, J.J. Bock, *et al*, *MNRAS* **313**, 559 (2000).
11. A.W. Blain, *et al*, *ASP Conf. Ser. Vol. 193*, 425 (2000).
12. J.J. Bock, *et al*, *Proc. SPIE* **3357**, 297 (1998).
13. S.C. Chapman, *et al*, *MNRAS* **in press**, astro-ph/9909092 (2000).
14. S.C. Chapman, *et al*, *MNRAS* **submitted**, (2001).
15. D.L. Clements, *et al*, *MNRAS* **256**, P35 (1992).
16. J.J. Condon, *ARA&A* **30**, 575 (1992).
17. C.D. Dowell, S.H. Moseley Jr., *et al*, *ASP Conf. Ser.*, **in press** (2000).
18. D. Downes, *et al*, *A&A* **347**, 809 (1999).
19. J.S. Dunlop, D.H. Hughes, *et al*, *Nature* **370**, 437 (1994).
20. L. Dunne, *et al*, *MNRAS* **315**, 115 (2000).

21. S.A. Eales, *et al*, MNRAS **in press**, (2000).
22. S.A. Eales, *et al*, ApJ **515**, 518 (1999).
23. A. Efstathiou, M. Rowan-Robinson, *et al*, MNRAS **313**, 734 (2000)
24. N. Erickson, this volume (2001).
25. D.P. Finkbeiner, M. Davis, *et al*, ApJ **in press**, astro-ph/0004175 (2000).
26. D.T. Frayer, R.J. Ivison, N.Z. Scoville, *et al*, ApJ **506**, L7 (1998).
27. D.T. Frayer, R.J. Ivison, N.Z. Scoville, *et al*, ApJ **514**, L13 (1999).
28. D.T. Frayer, I. Smail, *et al*, AJ **in press**, astro-ph/0005239 (2000).
29. W.K. Gear, *et al*, MNRAS **in press**, astro-ph/0007054 (2000).
30. J. Glenn, *et al*, Proc. SPIE **3357**, 326 (1998).
31. B. Guiderdoni, E. Hivon, F.R. Bouchet, *et al*, MNRAS **295**, 877 (1998).
32. B. Guiderdoni, and J.E.G. Devriendt, astro-ph/9911162, (2000).
33. M.G. Hauser, *et al*, ApJ **508**, 25 (1998).
34. W.S. Holland, *et al*, MNRAS **303**, 659 (1998).
35. <http://www.jach.hawaii.edu/JACpublic/JCMT/scuba/scuba2>.
36. D. Hughes, *et al*, Nature **394**, 241 (1998).
37. K.G. Isaak, R.G. McMahon, *et al*, MNRAS **269**, L28 (1994).
38. K.G. Isaak, A. Harris, and J. Zmuidzinas, BAAS **191**, 0911 (1997).
39. K.G. Isaak, *et al*, this volume (2001).
40. R.J. Ivison, I. Smail, J.-F. Le Borgne, *et al*, MNRAS **298**, 583 (1998).
41. R.J. Ivison, I. Smail, A.J. Barger, *et al*, MNRAS **315**, 209 (2000).
42. G.F. Lewis, S.C. Chapman, R.A. Ibata, *et al*, ApJ **505**, L1 (1998).
43. S.J. Lilly, *et al*, ApJ **518**, 641 (1999).
44. S.J. Lilly, *et al*, this volume (2001).
45. U. Lisenfeld, K.G. Isaak, and R.E. Hills, MNRAS **312**, 433 (2000).
46. T.G. Phillips, ESA SP-401, 223 (1997).
47. J.-L. Puget, *et al*, A&A **308**, L5 (1996).
48. M. Rowan-Robinson, MNRAS **316**, 885 (2000).
49. D.J. Schlegel, D.P. Finkbeiner and M. Davis, ApJ **500**, 525 (1998).
50. F.P. Schloerb, Proc. IAU **170**, 221 (1997).
51. I. Smail, R.J. Ivison and A.W. Blain, ApJ **490**, L5 (1997).
52. I. Smail, R.J. Ivison, J.-P. Kneib, *et al*, MNRAS **308**, 1061 (1999).
53. I. Smail, R.J. Ivison, A.W. Blain, *et al*, ApJ **507**, L21 (1998).
54. I. Smail, R.J. Ivison, *et al*, this volume, astro-ph/0008237 (2001).
55. G. Soucail, J.-P. Kneib, J. Bézecourt, *et al*, A&A **343**, L70 (1999).
56. N. Trentham, A.W. Blain and J. Goldader, MNRAS **305**, 61 (1999).
57. P. van der Werf, *et al*, this volume (2001).
58. D.J. Wilner and M.C.H. Wright, ApJ **488**, L67 (1997).
59. D.J. Wilner, *et al*, this volume (2001).
60. A. Wootten, ed. *Science with ALMA*, ASP Conf. Ser., in press (2000).